

On the distributions of wave periods, wavelengths, and amplitudes in a random wave field

Delun Xu, Xiang Li, Lizhen Zhang, Ning Xu, and Hongmin Lu

Physical Oceanography Laboratory, Ocean University of China, Qingdao, China

Received 29 July 2003; revised 29 February 2004; accepted 18 March 2004; published 14 May 2004.

[1] On the basis of a narrow-band Gaussian process, two theoretical probability density functions (PDFs) are derived by applying an approximate Hilbert transform to the process represented by a general form. The first PDF is for the joint distribution of the wave period τ and amplitude ρ of sea waves. It has the same merits as the PDF previously derived by *Longuet-Higgins* [1983], in being asymmetric in τ and depending only on the spectral width parameter ν , but gains an advantage that it predicts an exactly Rayleigh distribution of ρ and so facilitates its handling in theory and application in practice. In virtue of the advantage, a relatively simple conditional PDF of τ assuming ρ is derived, which may be used to predict an arbitrarily defined characteristic conditional wave period assuming the wave height from the average wave period. The second PDF is for the joint distribution of wavelengths and amplitudes in a unidirectional Gaussian wave field with narrow spectrum. It has the same form as the first PDF but depends only on the parameter μ defined by $\mu^2 = m_0 m_4 / m_2^2 - 1$, where m_n is the n th moment of spectrum. From this joint PDF, a PDF for the distribution of wavelengths of sea waves is also derived. Numerical simulation and laboratory experiments of wind waves and their results are reported. It is shown that the PDFs derived in this paper give fairly good fits to the simulated data and suitably filtered laboratory data.

INDEX TERMS: 0624 Electromagnetics: Guided waves; 3384 Meteorology and Atmospheric Dynamics: Waves and tides; 4263 Oceanography: General: Ocean prediction;
KEYWORDS: joint probability of wave variables, Hilbert transform, experiment

Citation: Xu, D., X. Li, L. Zhang, N. Hu, and H. Lu (2004), On the distributions of wave periods, wavelengths, and amplitudes in a random wave field, *J. Geophys. Res.*, 109, C05016, doi:10.1029/2003JC002073.

1. Introduction

[2] The statistical distributions of periods, wavelengths and amplitudes of sea waves have long been interesting due to their great importance to marine science. For them many theoretical probability density functions (PDFs hereinafter) have proposed in the last century.

[3] As early as in 1950s, *Longuet-Higgins* [1952, 1957] proposed the Rayleigh PDF for the distribution of sea-wave amplitudes, based on the envelope theory of Gaussian noise which had been developed in studying electric communication [*Rice*, 1945]. The Rayleigh PDF of amplitudes has been widely employed for many theoretical and practical purposes in marine studies. Also in this period, *Cartwright and Longuet-Higgins* [1956] derived a theoretical PDF of the maximum in a narrow-band Gaussian process. This PDF has also been applied in many fields of marine science. For example, it has been employed by *Srokosz* [1986] to develop a simple model for the probability of wave breaking in deep water.

[4] In the 1970s, many attentions were paid to the joint distribution of sea wave periods and amplitudes due to

requirements in marine science. *Lindgren* [1972] proposed an approximation to the joint PDF of wavelength and amplitude (defined as the differences in time and height between a maximum and the following minimum) in a Gaussian process, but the resulting expression requires a great deal of computation to evaluate and involves high moments of spectrum. *Longuet-Higgins* [1975] derived a PDF for the joint distribution of wave periods and amplitudes, based on a narrow-band approximation applied to the linear theory of Gaussian noise; its expression depends only on the spectral width ν , where $\nu^2 = m_0 m_2 / m_1^2 - 1$ with m_n as the n th moment of spectrum. While giving a fairly good fit to sea wave data with a narrow spectrum, this PDF failed in accounting for the observed asymmetry in the distribution of wave periods [e.g., *Goda*, 1978; *Chakrabarti and Cooley*, 1977]. Later, also based on a narrow-band Gaussian process, *Cavanié et al.* [1976] proposed another joint PDF, which accounts successfully for the asymmetry in the distribution of wave periods but involves the fourth moment of spectrum, m_4 , and therefore is inconvenient for practical purposes, for m_4 depends rather critically on the behavior of spectrum at high frequencies and it is inexistence to currently used spectral models of sea waves, such as the well-known JONSWAP spectrum and Pierson-Moscowitz spectrum. A lengthy and somewhat more accurate approx-

imation to the joint PDF of wavelength and amplitude in a Gaussian process was given by *Lindgren and Rychlik* [1982], but the resulting expression also depends on m_4 .

[5] To overcome the difficulties existing in the above mentioned joint PDFs of wave period and amplitude, *Longuet-Higgins* [1983] improved the joint PDF in the work of *Longuet-Higgins* [1975] by introducing a normalization factor $L(\nu)$, to take account of the fact that only positive values of wave period should be considered. The improved PDF is asymmetric in the distribution of wave periods and depends only on ν . However, this improvement is merely a mathematical treatment, which leads to a drawback that the resulting PDF predicts a slightly non-Rayleigh distribution of amplitudes, rather than the well-known Rayleigh one as it is under the linear theory of Gaussian process. Although this drawback is not significant for usual purposes, it may bring about some difficulties or inconveniences in further theoretical handling and practical applications of the PDF, as will be pointed out subsequently.

[6] Few theoretical PDFs have been proposed for the joint distribution of wavelengths and amplitudes and the distribution of wavelengths. This is perhaps because the wavelength of sea waves is a spatially two-dimensional variable and its direct measurement is difficult. *Sun* [1988] derived a joint PDF of four variables: amplitude, frequency, and wave numbers (in x and y directions), based on the ray theory of waves and a Fourier model of three-dimensional random wave field (an extension of the model for the surface elevation at a fixed point presented by *Longuet-Higgins* [1975]). The parameters in this joint PDF are expressed in terms of a determinant consisting of the correlations between these variables. From this joint PDF, a joint PDF of wavelength and amplitude may be derived, but the related analysis is difficult and the resulting expression depends on the directional spectrum of sea wave.

[7] The effect of nonlinearities on the statistical distributions of sea wave variables has been investigated empirically and theoretically by a number of researchers [e.g., *Cox and Munk*, 1954; *Longuet-Higgins*, 1963; *Huang and Long*, 1980; *Huang et al.*, 1983; *Tayfun*, 1980; *Srokosz*, 1986]. However, these investigations concentrated upon the non-linear effect on the distributions of sea surface elevations and slopes, and scarcely involved the distributions of wave periods, wavelengths and amplitudes.

[8] The purpose of this paper is to present an alternative theoretical joint PDF of wave period and amplitude in a narrow-band Gaussian process and a theoretical joint PDF of wavelength and amplitude in a unidirectional Gaussian wave field of narrow-band. In section 2 we shall give the derivation of the former, in which an approximate Hilbert transform will be applied; the resulting joint PDF has the same merits as that in the work of *Longuet-Higgins* [1983] but predicts an exactly Rayleigh distribution of amplitudes. In accordance with this joint PDF, conditional distributions of wave periods assuming the amplitude will be examined in detail. The derivation of the joint PDF of wavelength and amplitude will be given in section 3, in which the approximate Hilbert transform will also be applied; the resulting joint PDF depends only on the parameter μ , where $\mu^2 = m_0 m_4 / m_2^2 - 1$. From this joint PDF, a PDF of wavelength depending only on the parameter μ will be derived. Section 4 will report numerical simulation and laboratory experiments

performed in a wind-wave flume. Their results well support the theoretical PDFs derived in this paper. Some conclusions will be drawn in the final section.

2. Joint Distribution of Wave Periods and Amplitudes

2.1. Joint Probability Density Function (PDF)

[9] As in the work of *Longuet-Higgins* [1975, 1983], we begin with the representation of the sea surface elevation $\zeta(t)$ in the form

$$\left. \begin{aligned} \zeta(t) &= \text{Re} A(t) e^{i\bar{\omega}t} \\ A(t) &= \rho(t) e^{i\phi(t)} \end{aligned} \right\} \quad (1)$$

where $\bar{\omega}$ is the carrier frequency, and the phase $\phi(t)$ and local amplitude $\rho(t)$ are both real and slowly varying functions of the time t . Let

$$\varphi(t) = \phi(t) + \bar{\omega}t. \quad (2)$$

It follows from equation (1) that

$$\zeta(t) = \text{Re} \rho(t) e^{i\varphi(t)}. \quad (3)$$

We also adopt the narrow-band hypothesis, namely,

$$\nu^2 = \frac{m_0 m_2}{m_1^2} - 1 \ll 1, \quad (4)$$

where m_n denotes the n th moment of the one-sided spectrum $s(\omega)$ of $\zeta(t)$, defined as

$$m_n = \int_0^\infty \omega^n s(\omega) d\omega. \quad (5)$$

Longuet-Higgins [1957] has shown that the variance of the change rate $\dot{\rho}(t)$ (a dot denotes differentiation with respect to t , hereinafter) is proportional to ν^2 . This implies that by the hypothesis (4), $\dot{\rho}(t)$ is negligible in comparison with $\zeta(t)$. In this case the Hilbert transform of $\zeta(t)$, which is defined as

$$\xi(t) = \frac{1}{\pi} \int_{-\infty}^{+\infty} \frac{\zeta(\tau)}{t - \tau} d\tau = \zeta(t) * \frac{1}{\pi t}, \quad (6)$$

can be approximated as

$$\xi(t) = \text{Im} \rho(t) e^{i\varphi(t)} \quad (7)$$

since the Hilbert transform is a quadrature transform [see, e.g., *Papoulis*, 1984].

[10] It follows from equations (3) and (7) that

$$\rho(t) = [\zeta^2(t) + \xi^2(t)]^{1/2} \quad (8)$$

and

$$\varphi(t) = \arctan \left[\frac{\xi(t)}{\zeta(t)} \right]. \quad (9)$$

[11] It is worthwhile noting that the Hilbert transform technique has been extensively and effectively employed to

measure the local wave variables from a wave record with narrow-spectrum [Melville, 1983; Bitner-Gregersen and Gran, 1983; Shum and Melville, 1984; Hwang et al., 1989; Stansell and MacFanlane, 2002].

[12] We further assume that $\zeta(t)$ is a stationary Gaussian process. As $\xi(t)$, $\dot{\zeta}(t)$ and $\dot{\xi}(t)$ are all linear transforms of $\zeta(t)$, they are jointly stationary Gaussian and their joint PDF can therefore be expressed as

$$f(\varsigma, \xi, \dot{\zeta}, \dot{\xi}) = \frac{1}{(2\pi)^2 D^{1/2}} \left\{ -\frac{1}{2D} \sum_{i=1}^4 \sum_{j=1}^4 D_{ij} x_i x_j \right\}, \quad (10)$$

where

$$x_1 = \varsigma, x_2 = \xi, x_3 = \dot{\zeta}, x_4 = \dot{\xi}, \quad (11)$$

$$D = \begin{pmatrix} R_{11} & R_{12} & R_{13} & R_{14} \\ R_{21} & R_{22} & R_{23} & R_{24} \\ R_{31} & R_{32} & R_{33} & R_{34} \\ R_{41} & R_{42} & R_{43} & R_{44} \end{pmatrix}, \quad (12)$$

and D_{ij} is the residual subdeterminant of D with regard to R_{ij} , with R_{ij} defined as

$$R_{ij} = \overline{x_i(t)x_j(t)},$$

where the over line denotes the assembly average, namely, the expected value.

[13] Calculating R_{ij} , D_{ij} and D in equation (10) from equations (3) and (7) and transforming $f(\varsigma, \xi, \dot{\zeta}, \dot{\xi})$ into $f(\rho, \varphi, \dot{\rho}, \dot{\varphi})$ (see Appendix A) we have the joint PDF of $\rho(t)$ and $\dot{\varphi}(t)$

$$f(\rho, \dot{\varphi}) = \frac{\rho^2}{(2\pi m_0 \Delta)^{1/2}} \exp \left\{ -\frac{\rho^2}{2\Delta} (m_2 + m_0 \dot{\varphi}^2 - 2m_1 \dot{\varphi}) \right\}, \quad (13)$$

where

$$\Delta = (m_0 m_2 - m_1^2)^{1/2}. \quad (14)$$

[14] The local wave period $\tau(t)$ is defined as

$$\tau(t) = \frac{2\pi}{|\omega(t)|}, \quad (15)$$

where $\omega(t) = \dot{\varphi}(t)$ is the local radian frequency. Introducing the normalized amplitude $R(t)$ and wave period $T(t)$:

$$R(t) = \frac{\rho(t)}{(2m_0)^{1/2}}, \quad (16)$$

$$T(t) = \frac{\tau(t)}{2\pi m_0 / m_1}, \quad (17)$$

as in the work of Longuet-Higgins [1983], we have from equation (13) the joint PDF of $R(t)$ and $T(t)$

$$f(R, T) = \frac{\pi^{3/2} R^2}{8\nu T^2} \left(1 + \exp \left\{ -\frac{\pi R^2}{4\nu^2 T} \right\} \right) \cdot \exp \left\{ -\frac{\pi^2 R^2}{16} \left[1 + \frac{1}{\nu^2} \left(1 - \frac{1}{T} \right)^2 \right] \right\}, \quad (18)$$

which differs in expression apparently from the joint PDF in the work of Longuet-Higgins [1983]:

$$f_{LH}(R, T) = \frac{2R^2}{\pi^{1/2} \nu T^2} \exp \left\{ -R^2 \left[1 + \frac{1}{\nu^2} \left(1 - \frac{1}{T} \right)^2 \right] \right\} L(\nu) \left. \vphantom{\frac{2R^2}{\pi^{1/2} \nu T^2}} \right\} \frac{1}{L(\nu)} = \frac{1}{2} \left[1 + (1 + \nu^2)^{-1/2} \right] \quad (19)$$

However the numerical difference between $f(R, T)$ and $f_{LH}(R, T)$ is very slight, as can be seen from Figures 1a and 1b which show the contours of $f(R, T)/f_{\max}$ and $f_{LH}(R, T)/f_{LH\max}$, respectively, for a sequence of values of ν , where f_{\max} denotes maximum or mode of the PDF found from the condition that $\frac{\partial f}{\partial R}$ and $\frac{\partial f}{\partial T}$ both vanish.

[15] We note that the difference between equations (18) and (19) is because equation (18) is directly derived from a Gaussian process under the hypothesis $\nu^2 \ll 1$, whereas equation (19) is obtained by introducing the normalization factor $L(\nu)$ to improve Longuet-Higgins' [1975] PDF whose derivation involved the approximation

$$T(t) = \frac{2\pi}{\bar{\omega} + \dot{\phi}(t)} \approx \frac{2\pi}{\bar{\omega}} \left[1 - \frac{\dot{\phi}(t)}{\bar{\omega}} \right].$$

It is this approximation that makes the resulting joint PDF symmetric in T [see also Shum and Melville, 1984], though such a approximation is legitimate to order ν and its effect on the PDF is slight in magnitude.

[16] To further compare equations (18) and (19) we refer to $h(t) = 2\rho(t)$ as the local wave height and define the normalized wave height as

$$H(t) = \frac{h(t)}{(2\pi m_0)^{1/2}}. \quad (20)$$

Combining equations (20) and (16) we have

$$H(t) = \frac{2}{\pi^{1/2}} R(t). \quad (21)$$

Thus the PDFs (18) and (19) can be transformed into the forms

$$f(H, T) = \frac{\pi H^2}{4\nu T^2} \exp \left\{ -\frac{\pi H^2}{4} \left[1 + \frac{1}{\nu^2} \left(1 - \frac{1}{T} \right)^2 \right] \right\} G(H, T; \nu) \left. \vphantom{\frac{\pi H^2}{4\nu T^2}} \right\} G(H, T; \nu) = 1 + \exp \left\{ -\frac{\pi H^2}{\nu^2 T} \right\} \quad (22)$$

$$f_{LH}(H, T) = \frac{\pi H^2}{4\nu T^2} \exp \left\{ -\frac{\pi H^2}{4} \left[1 + \frac{1}{\nu^2} \left(1 - \frac{1}{T} \right)^2 \right] \right\} L(\nu). \quad (23)$$

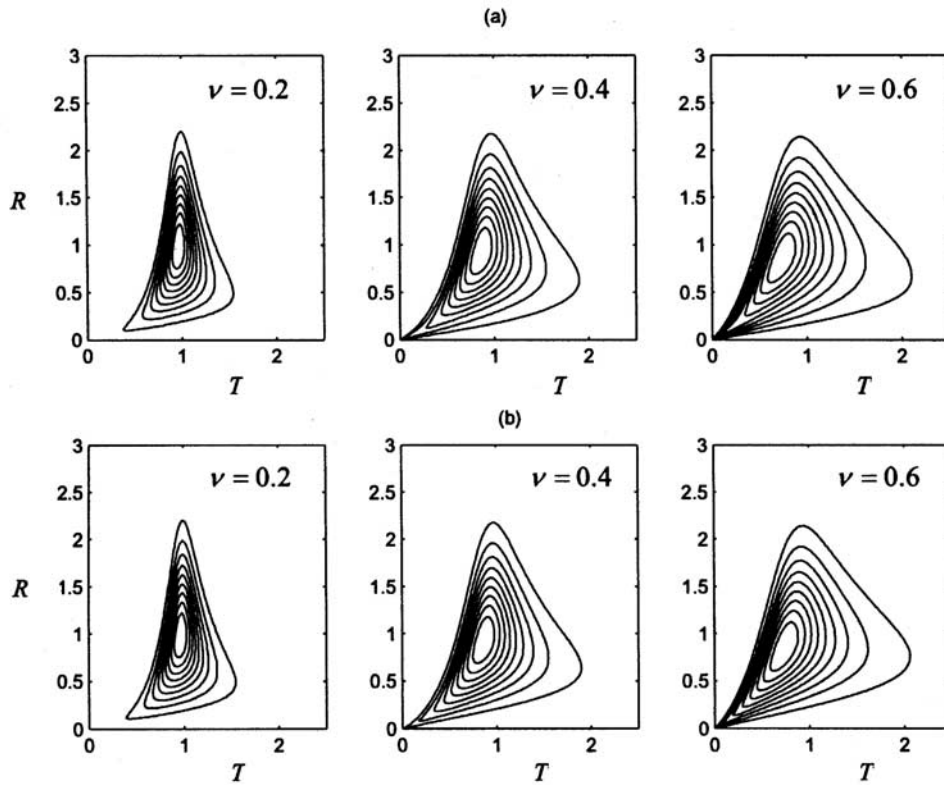


Figure 1. Contours of (a) $f(R, T)/f_{\max}$ and (b) $f_{LH}(R, T)/f_{LH\max}$ given by equations (18) and (19), respectively; f/f_{\max} and $f_{LH}/f_{LH\max}$ take the values 0.1, 0.2,, 0.9, respectively, from the center outward.

Clearly, the difference between $f(H, T)$ and $f_{LH}(H, T)$ manifests itself only by that between $G(H, T; \nu)$ and $L(\nu)$. We note that $G(H, T; \nu)$ results from the rigorous derivation based on a narrow-band Gaussian process, whereas $L(\nu)$ is a normalization factor introduced to improve the PDF in the work of *Longuet-Higgins* [1975].

[17] A striking difference between $f(R, T)$ and $f_{LH}(R, T)$ is that the PDF of $R(t)$ predicted by $f(R, T)$ is exactly Rayleigh:

$$f(R) = 2R \exp\{-R^2\}, \quad (24)$$

as it is under linear theory of Gaussian process [*Longuet-Higgins*, 1952, 1957], whereas that predicted by $f_{LH}(R, T)$ is slightly non-Rayleigh:

$$\left. \begin{aligned} f_{LH}(R) &= 2RL(\nu) \exp\{-R^2\} \operatorname{erf}(R/\nu) \\ \operatorname{erf}(R/\nu) &= \frac{1}{\sqrt{\pi}} \int_{-\infty}^{R/\nu} e^{-\beta^2} d\beta \end{aligned} \right\}, \quad (25)$$

where $\operatorname{erf}(\cdot)$ represents the well-known error function. *Longuet-Higgins* [1983] has shown that for any values of ν the numerical difference between $f(R)$ and $f_{LH}(R)$ is slight. However, $f(R)$ is much simpler and easier to handle and apply than $f_{LH}(R)$, especially in examining the conditional distribution of wave periods assuming the wave height, as will be seen subsequently.

2.2. Discussion

[18] Traditionally the wave period and wave height in a wave signal are defined as the time duration and maximum

height between two successive up-zero-crossings (such wave variables are referred to as the zero-crossing ones), whereas what we deal with here are the local variables, which in practice take values at points uniformly spaced at time intervals of Δt . It is pertinent to inquire whether or under what condition the distribution of a zero-crossing variable is equivalent to that of its corresponding local variable. We have adopted the narrow-band hypothesis, $\nu^2 \ll 1$. This ensures that the change rate of envelope, $\dot{\rho}(t)$, is much less than that of surface elevation, $\dot{\zeta}(t)$, and the wave crests lie almost on the envelope $\zeta(t) = \rho(t)$ [*Longuet-Higgins*, 1983]. Under this condition, the distribution of a local variable is almost equivalent to that of its corresponding zero-crossing variable.

[19] As reasoned in the preceding derivation, equation (7) is a pertinent approximation to the Hilbert transform of $\zeta(t)$ under the hypothesis $\nu^2 \ll 1$. This means that this approximation is correct only to order ν . One would inquire how the distribution is when the approximation is correct to order ν^2 . Such an approximation means that the process under consideration is of nonnarrow band. *Cartwright and Longuet-Higgins* [1956] have shown that for a Gaussian process, the occurrence probability of negative maxima increases with spectral width. This implies that a nonnarrow band Gaussian process has many maxima other than crests, and a part of these maxima are even less than the mean of the process, namely, below the mean level of the process. Such being the case the wave period and wave height are hard to define. Perhaps just because of this, *Lindgren* [1972] and *Lindgren and Rychlik* [1982] had to propose somewhat

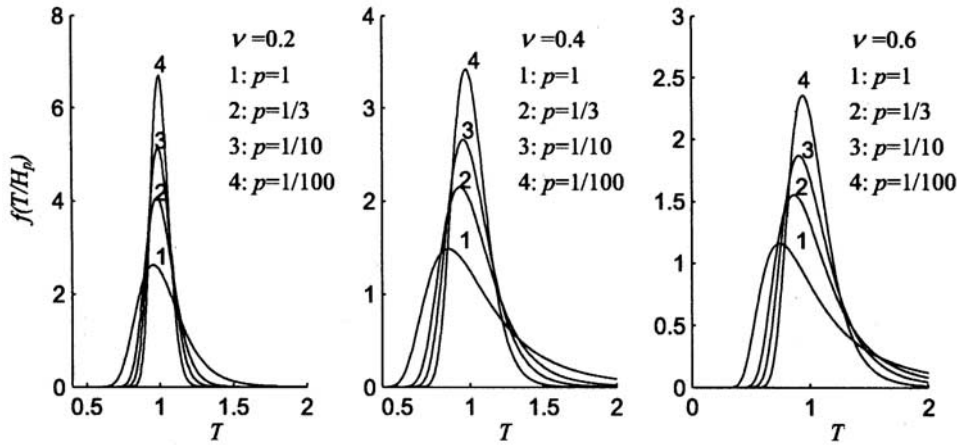


Figure 2. The conditional distributions of T assuming $H = H_1, H_{1/3}, H_{1/10}$ and $H_{1/100}$ given by equation (33) together with equation (34) for $\nu =$ (a) 0.2, (b) 0.4 and (c) 0.6.

new variables called the wavelength and amplitude which are defined as the differences in time and height between a maximum and the following minimum, and gave some lengthy approximations. This leads to that the resulting joint PDF depends on the parameter ε involving m_4 , and requires a great deal of computation to evaluate. In fact, as pointed out by *Longuet-Higgins* [1983], observational evidences have suggested that further corrections of order ν^2 are small and not very significant for practical applications.

2.3. Conditional Distribution of Wave Periods

[20] *Longuet-Higgins* [1983] has partly examined the conditional distribution of $T(t)$ in terms of $f_{LH}(T)$. As the present PDF $f(R, T)$ predicts an exactly Rayleigh PDF of $R(t)$, this makes it advantageous to further examining the conditional distribution and giving some useful results. For convenience, we shall adopt the PDF $f(H, T)$ given in equation (22) that is equivalent to $f(R, T)$ in equation (18).

[21] The total PDF of $H(t)$ given by $f(H, T)$ is

$$f(H) = \frac{\pi}{2} H \exp\left\{-\frac{\pi}{4} H^2\right\}. \tag{26}$$

The conditional PDF of $T(t)$ assuming $H(t), f(T|H)$, is found by

$$f(T | H) = \frac{f(H, T)}{f(H)}. \tag{27}$$

Insertion of equations (22) and (26) in equation (27) gives

$$f(T | H) = \frac{H}{2\nu T^2} \left(1 + \exp\left\{-\frac{\pi H^2}{\nu^2 T}\right\}\right) \exp\left\{-\frac{\pi H^2}{4\nu^2} \left(1 - \frac{1}{T}\right)^2\right\}. \tag{28}$$

On the other hand, equation (26) gives the PDF of local wave height $h(t) = 2\rho(t)$ as

$$f(h) = \frac{h}{4m_0} \exp\left\{-\frac{h^2}{8m_0}\right\}, \tag{29}$$

and then the average wave height \bar{h} is related to m_0 by

$$\bar{h} = \int_0^\infty hf(h)dh = (2\pi m_0)^{1/2}. \tag{30}$$

[22] Let h_p denote the value of wave height averaged over the p fraction highest waves, that is,

$$\left. \begin{aligned} h_p &= \frac{1}{p} \int_{h_0}^\infty hf(h)dh \\ p &= \int_{h_0}^\infty f(h)dh \end{aligned} \right\}, \tag{31}$$

where h_0 is the p quantile, namely, such a value of wave height that the accumulative probability of waves with wave height exceeding the value is p ; $h_{1/3}$ is well known as the significant wave height. Normalizing h_p as

$$H_p = \frac{h_p}{\bar{h}} = \frac{h_p}{(2\pi m_0)^{1/2}}, \tag{32}$$

we have from equation (28) the conditional PDF of $T(t)$ assuming $H(t) = H_p$,

$$f(T | H_p) = \frac{H_p}{2\nu T^2} \left(1 + \exp\left\{-\frac{\pi H_p^2}{\nu^2 T}\right\}\right) \exp\left\{-\frac{\pi H_p^2}{4\nu^2} \left(1 - \frac{1}{T}\right)^2\right\}. \tag{33}$$

Further, H_p can be expressed as a function of p by inserting equation (29) in equation (31) and using equations (30) and (32):

$$H_p = \left(\frac{4}{\pi} \ln \frac{1}{p}\right)^{1/2} + \frac{1}{p} \left\{1 - \operatorname{erf} \left[\left(\ln \frac{1}{p}\right)^{1/2}\right]\right\}, \tag{34}$$

as has been given in the work of *Longuet-Higgins* [1952]. Several typical results given by equation (34) are as follows:

$$H_1 = 1, H_{1/3} = 1.598, H_{1/10} = 2.032, H_{1/100} = 2.663. \tag{35}$$

[23] Figure 2 shows the conditional distributions of T assuming $H = H_1, H_{1/3}, H_{1/10}$ and $H_{1/100}$ given by equations (33) and (34) for $\nu = 0.2, 0.4$ and 0.6 , respectively. It may be of interest for ocean engineering and others to find a relationship between a characteristic conditional

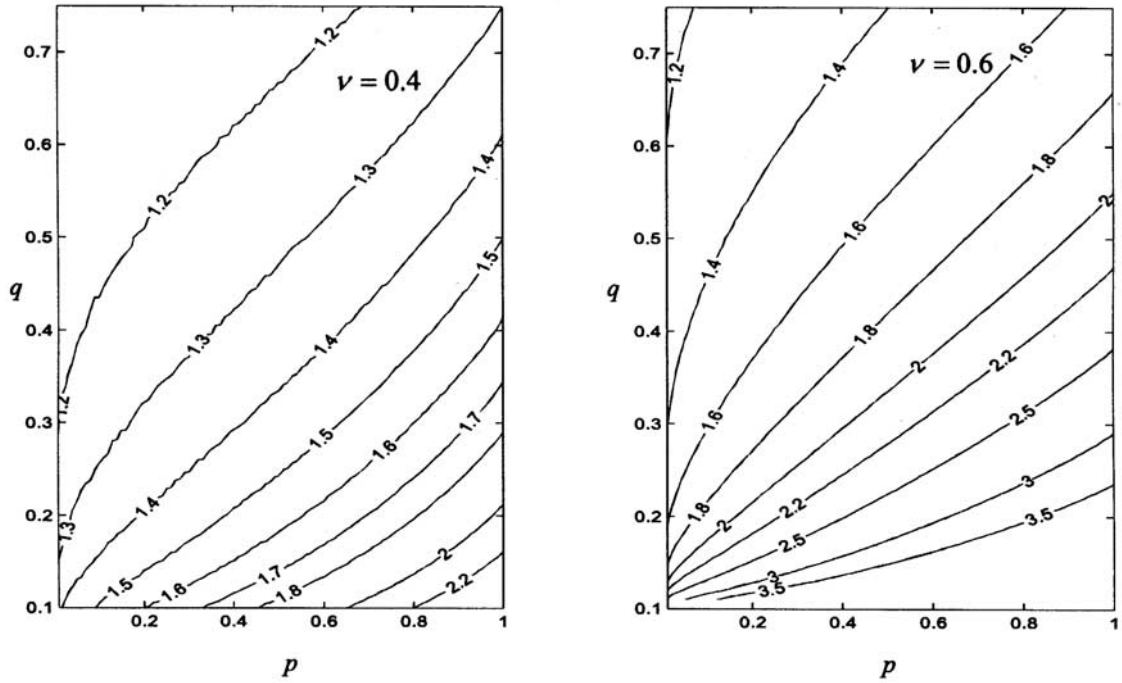


Figure 3. Counters of \bar{T}_{pq} computed from equation (41) together with equations (33) and (34) for (left) $\nu = 0.4$ and (right) $\nu = 0.6$.

wave period and the average wave period $\bar{\tau}$, so as to predict the former from $\bar{\tau}$. We shall define two kinds of characteristic conditional wave periods and derive such relationships in terms of $f(T|H_p)$ shown in equation (33).

[24] First, we define the characteristic conditional wave period $\bar{\tau}_{pq}$ by

$$\left. \begin{aligned} \bar{\tau}_{pq} &= \frac{1}{q} \int_{\tau_0}^{\infty} \tau f(\tau | h_p) d\tau \\ q &= \int_{\tau_0}^{\infty} f(\tau | h_p) d\tau \end{aligned} \right\}, \quad (36)$$

where $f(\tau|h_p)$ is the conditional PDF of τ assuming $h = h_p$, and τ_0 is such a value of $\tau(t)$ that the accumulative probability of waves with $h(t) = h_p$ and $\tau(t) \geq \tau_0$ is q . In other words, $\bar{\tau}_{pq}$ is the wave period averaged over the q fraction longest waves with wave heights equaling the identical value h_p . It is easy to see from equation (36) that $q = 1$ when $\tau_0 = 0$. In this case

$$\bar{\tau}_{p,1} = \int_0^{\infty} \tau f(\tau | h_p) d\tau \quad (37)$$

is the wave period averaged over all of the waves with wave height equaling h_p . In the extreme case, $p = 1$ and $q = 1$, we have

$$\bar{\tau}_{1,1} = \bar{\tau}.$$

[25] Longuet-Higgins [1975] has shown that for a narrow-band Gaussian process, $\bar{\tau}$ can be approximated as

$$\bar{\tau} = \frac{2\pi m_0}{m_1}, \quad (38)$$

so that the normalized wave period $T(t)$ can be rewritten as

$$T(t) = \frac{\tau(t)}{\bar{\tau}}. \quad (39)$$

Normalizing $\bar{\tau}_{pq}$ and τ_0 as

$$\bar{T}_{pq} = \frac{\bar{\tau}_{pq}}{\bar{\tau}} \quad \text{and} \quad T_0 = \frac{\tau_0}{\bar{\tau}}, \quad (40)$$

we have

$$\left. \begin{aligned} \bar{T}_{pq} &= \frac{\bar{\tau}_{pq}}{\bar{\tau}} = \frac{1}{q} \int_{T_0}^{\infty} T f(T | H_p) dT \\ q &= \int_{T_0}^{\infty} f(T | H_p) dT \end{aligned} \right\}. \quad (41)$$

[26] This is the relationship between $\bar{\tau}_{pq}$ and $\bar{\tau}$ expressed in terms of $f(T|H_p)$. Inserting equations (33) and (34) into equation (41) and numerically evaluating the integrals we obtain values of \bar{T}_{pq} for different p , q and ν . Figure 3 shows contours of \bar{T}_{pq} for $\nu = 0.4$ and 0.6 . The relation between $\bar{\tau}_{p_1q_1}$ and $\bar{\tau}_{p_2q_2}$ can be found from

$$\frac{\bar{\tau}_{p_1q_1}}{\bar{\tau}_{p_2q_2}} = \frac{\bar{T}_{p_1q_1}}{\bar{T}_{p_2q_2}}. \quad (42)$$

[27] It may be interesting to discuss another kind of characteristic conditional wave periods, $\tilde{\tau}_p$, defined by

$$\left. \frac{\partial f(\tau | h_p)}{\partial \tau} \right|_{\tau=\tilde{\tau}_p} = 0. \quad (43)$$

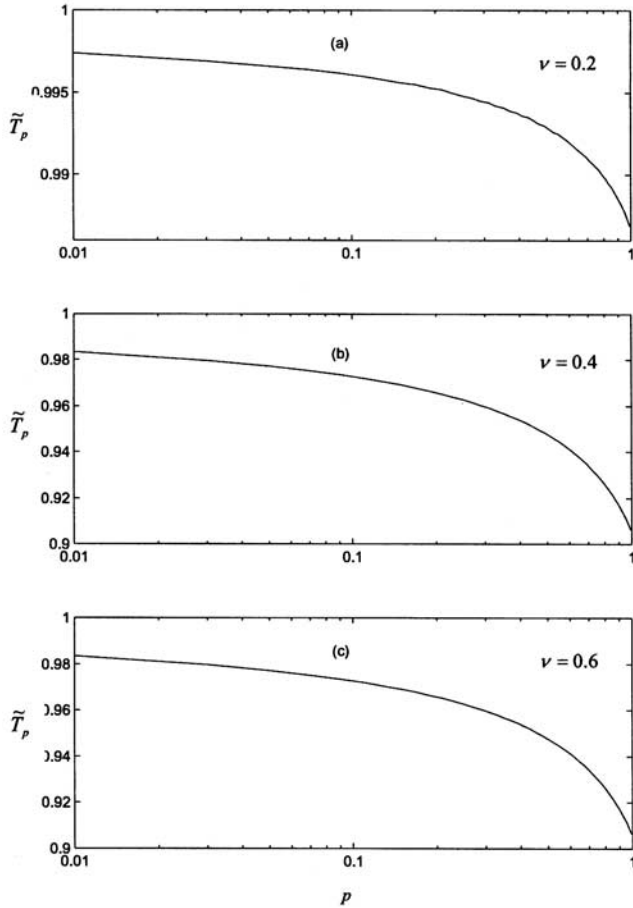


Figure 4. \tilde{T}_p versus p given by equation (44) together with equations (33) and (34) for (a) $\nu = 0.2$, (b) 0.4 , and (c) 0.6 .

In other words, $\tilde{\tau}_p$ is the most probable wave period of the waves with wave heights equaling h_p . The normalization counterpart of equation (43) is

$$\left. \frac{\partial f(T|H_p)}{\partial T} \right|_{T=\tilde{\tau}_p} = 0, \tag{44}$$

where

$$\tilde{T}_p = \frac{\tilde{\tau}_p}{\bar{\tau}}. \tag{45}$$

Inserting equations (33) and (34) into equation (44) and numerically computing the differential we obtain values of \tilde{T}_p for different p and ν , which are shown in Figure 4.

2.4. Distribution of Wave Periods

[28] Integration of equation (22) with respect to H over $0 < H < \infty$ gives the PDF of the normalized wave period T

$$\left. \begin{aligned} f(T) &= \frac{1}{2\nu T^2} \left[1 + \frac{1}{\nu^2} \left(1 - \frac{1}{T} \right)^2 \right]^{-3/2} U(T; \nu) \\ U(T; \nu) &= \left[1 + \frac{\nu^2 + \left(1 - \frac{1}{T} \right)^2}{\nu^2 + \left(1 + \frac{1}{T} \right)^2} \right]^{3/2} \end{aligned} \right\}, \tag{46}$$

while the same integration of equation (23) gives [Longuet-Higgins, 1983]

$$f_{LH}(T) = \frac{1}{2\nu T^2} \left[1 + \frac{1}{\nu^2} \left(1 - \frac{1}{T} \right)^2 \right]^{-3/2} L(\nu). \tag{47}$$

Clearly, the difference between $f(T)$ and $f_{LH}(T)$ manifests itself only by that between $U(T; \nu)$ and $L(\nu)$.

[29] Figure 5 shows the distributions given by $f(T)$ and $f_{LH}(T)$, respectively, for a sequence of ν . As can be seen from the figure, the numerical difference between $f(T)$ and $f_{LH}(T)$ is very slight for all values of ν .

[30] The PDF of the wave period τ derived from equation (46), namely, the dimensional version of equation (46) is

$$f(\tau) = \frac{\pi(m_0^2 - m_1 m_2)\tau}{m_0^{1/2}(m_2 \tau^2 - 4\pi m_1 \tau + 4\pi^2 m_0)^{3/2}}. \tag{48}$$

It is easy to see that $f(\tau)$ is asymmetric and $f(\tau) = 0$ when $\tau = 0$. We shall provide some numerical simulation and laboratory experimental evidences for equation (48) in section 4.

3. Joint Distribution of Wavelengths and Amplitudes

3.1. Joint PDF of Wavelength and Amplitude

[31] For a unidirectional random wave field, we represent the surface elevation in the direction of wave progression in the form

$$\zeta(x, t) = \text{Re} \rho(x, t) e^{i\varphi(x, t)}. \tag{49}$$

We assume that the wave field is stationary in t and homogeneous in x . This allows us to confine concern to the statistics of wavelength at a given t . In this case, equation (49) can be simplified as

$$\zeta(x) = \text{Re} \rho(x) e^{i\varphi(x)}, \tag{50}$$

which is the same in form as equation (3) except for the substitution of t with x .

[32] Still we adopt the narrow-band hypothesis. As is similar to equation (4), here this hypothesis is characterized by

$$\mu^2 = \frac{M_0 M_2}{M_1^2} - 1 \ll 1, \tag{51}$$

where M_n is the n th moment of the wave number spectrum $N(k)$ (one-sided) of $\zeta(x)$, defined as

$$M_n = \int_0^\infty k^n N(k) dk. \tag{52}$$

By this hypothesis $\rho_x(x)$ is negligible in comparison with $\zeta_x(x)$ (a subscript x denotes differentiation with respect to x hereinafter), so that the Hilbert transform of $\zeta(x)$ defined as

$$\xi(x) = \frac{1}{\pi} \int_{-\infty}^{+\infty} \frac{\zeta(r)}{x-r} dr = \zeta(x) * \frac{1}{\pi x}, \tag{53}$$

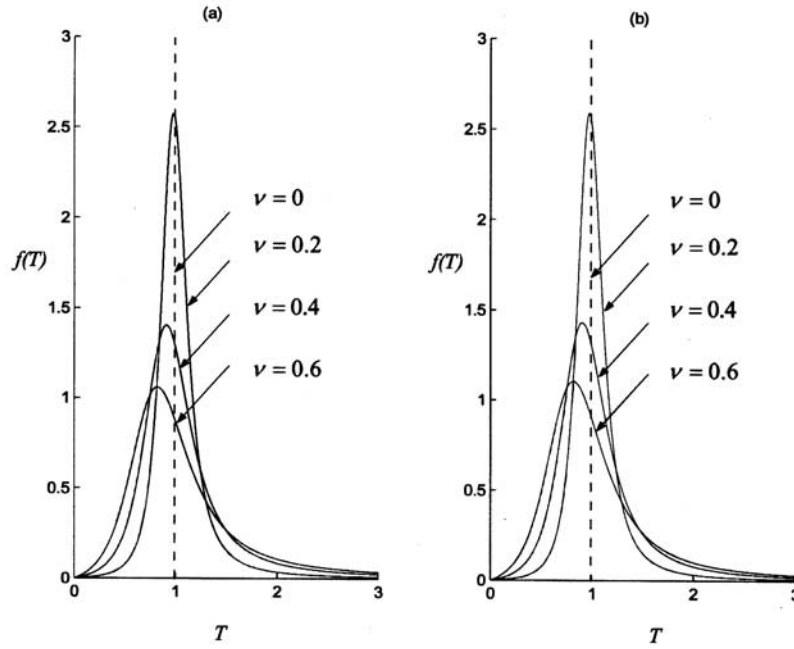


Figure 5. Comparison between (a) $f(T)$ and (b) $f_{LH}(T)$.

can be pertinently approximated as

$$\xi(x) = \text{Im} \rho(x) e^{i\varphi(x)}, \quad (54)$$

by reason similar to that of equation (7). It follows from equations (50) and (54) that

$$\rho(x) = [\varsigma^2(x) + \xi^2(x)]^{1/2} \quad (55)$$

$$\varphi(x) = \arctan \left[\frac{\xi(x)}{\varsigma(x)} \right]. \quad (56)$$

As $\xi(x)$, $\varsigma_x(x)$ and $\xi_{xx}(x)$ are all linear transforms of the Gaussian process $\varsigma(x)$, they are jointly Gaussian. Their joint PDF can thus be expressed as

$$f(\varsigma, \xi, \varsigma_x, \xi_x) = \frac{1}{(2\pi)^2 D^{1/2}} \left\{ -\frac{1}{2D} \sum_{i=1}^4 \sum_{j=1}^4 D_{ij} y_i y_j \right\}, \quad (57)$$

where $y_1 = \varsigma$, $y_2 = \xi$, $y_3 = \varsigma_x$ and $y_4 = \xi_x$,

$$D = \det |R_{ij}| \quad i, j = 1, 2, 3, 4, \quad (58)$$

with R_{ij} defined as

$$R_{ij} = \overline{y_i(x) y_j(x)}. \quad (59)$$

[33] Through a derivation parallel to that given in Appendix A, we obtain from equation (57) the joint PDF of $\rho(x)$ and $\varphi_x(x)$

$$f(\rho, \varphi_x) = \frac{\rho}{(2\pi M_0 \Gamma)^{1/2}} \exp \left\{ -\frac{\rho^2}{2\Gamma} (M_2 + M_0 \varphi_x^2 - 2M_1 \varphi_x) \right\}, \quad (60)$$

where

$$\Gamma = M_0 M_2 - M_1^2. \quad (61)$$

[34] The instantaneous wave number $k(x)$, wavelength $\lambda(x)$ and wave height $h(x)$ are defined as

$$k(x) = \varphi_x(x), \quad (62)$$

$$\lambda(x) = \frac{2\pi}{|k(x)|}, \quad (63)$$

$$h(x) = 2\rho(x), \quad (64)$$

and their normalized versions are defined as

$$K(x) = \frac{M_0}{M_1} k(x), \quad (65)$$

$$L(x) = \frac{\lambda(x)}{2\pi M_0 / M_1} = \frac{1}{|k(x)|}, \quad (66)$$

$$B(x) = \frac{h(x)}{(2\pi M_0)^{1/2}}. \quad (67)$$

After a derivation parallel to that of equation (22) we have from equation (60) the joint PDF of $B(x)$ and $L(x)$

$$f(B, L) = \frac{\pi B^2}{4\mu L^2} \left(1 + \exp \left\{ -\frac{\pi B^2}{\mu^2 L} \right\} \right) \cdot \exp \left\{ -\frac{\pi B^2}{4} \left[1 + \frac{1}{\mu^2} \left(1 - \frac{1}{L} \right)^2 \right] \right\}. \quad (68)$$

As is easy to see, this expression is formally the same as $f(H, T)$ given in equation (22) and their difference manifests itself only in implications of the variables and parameter. We shall not show the contours of $f(B, L)$ once again.

[35] Integration of equation (68) with respect to L over $0 < L < \infty$ gives the PDF of $B(x)$

$$f(B) = \frac{\pi}{2} B \exp\left\{-\frac{\pi}{4} B^2\right\}, \quad (69)$$

which is also exactly Rayleigh.

[36] It is convenient for practical application to express μ in terms of m_n that can be calculated from existing frequency-spectral models for sea waves, such as the well known Pierson-Moscowitz and JONSWAP spectra. In virtue of the dispersion relation for wave components under linear theory, $k = \omega^2/g$, we have from equation (52) that

$$M_n = \frac{1}{g^n} m_{2n}, \quad (70)$$

where g is the gravity acceleration. Thus

$$\mu = \left(\frac{m_0 m_4}{m_2^2} - 1\right)^{1/2}. \quad (71)$$

It is easy to show that

$$\mu^2 = \frac{\varepsilon^2}{1 - \varepsilon^2}, \quad (72)$$

where ε is the well-known spectral width parameter defined as

$$\varepsilon = \left(1 - \frac{m_2^2}{m_0 m_4}\right)^{1/2}$$

[Cartwright and Longuet-Higgins, 1956]. Obviously, $\mu \approx \varepsilon$ for $\varepsilon^2 \ll 1$.

[37] From equations (68) and (66) we have the PDF of instantaneous wavelength

$$f(\lambda) = \frac{\pi g \lambda (m_0 m_4 - m_2^2)}{m_0^{1/2} (m_4 \lambda^2 - 4 \pi g m_2 \lambda + 4 \pi^2 g^2 m_0)^{3/2}}, \quad (73)$$

which depends on m_4 in addition to m_0 and m_2 . For it we shall provide some experimental evidences in section 4.

3.2. Discussion

[38] In the derivation of $f(B, L)$, we adopted the narrow-band hypothesis, namely, $\mu^2 \ll 1$. This hypothesis ensure that $\rho_x(x)$ is much less than $\varsigma_x(x)$ and the wave crests lie almost on the envelope $\varsigma(x) = \rho(x)$. In this case the distribution of an instantaneous variable is almost equivalent to that of its corresponding spatial zero-crossing variable.

[39] As is clearly seen, the PDF (68) is formally identical to $f(H, L)$ given in equation (22), but the parameter μ , involving m_4 in addition to m_0 and m_2 , differs from ν , as can be seen from equation (71). This difference results from the dispersion relation $k = \omega^2/g$, by which the temporal variable

$\tau(t)$ is related to the spatial variable $\lambda(x)$ under linear theory of Gaussian process.

[40] Owing to the difficulty in directly measuring the wavelength both in laboratory and in the field, we have not been able to provide directly observational evidence for the PDF of wavelength shown in equation (73). However, we have measured the wavelength in laboratory with an indirect method and the measured results support the PDF to a great agree extent. This will be reported subsequently.

4. Experimental Evidences

[41] To evidence the PDFs proposed in this paper, we have performed three experiments: one numerical simulation experiment and two laboratory experiments.

4.1. Numerical Simulation Experiment

[42] As the PDFs derived in this paper are based on linear theory, we first test them by a linear numerical simulation experiment. With the Wallops spectrum for deep water [Huang *et al.*, 1981] as target, the surface elevation of random waves is simulated by using a linear filtering method. From the simulated signals we measure local wave amplitudes and periods and then compare their experimental distributions with the theoretical distributions derived in this paper.

[43] The wallops spectrum is expressed as

$$S(\omega) = \frac{\beta g^2}{\omega_p^5} \left(\frac{\omega_p}{\omega}\right)^m \exp\left\{-\frac{m}{4} \left(\frac{\omega_p}{\omega}\right)^4\right\}. \quad (74)$$

To be close to the condition of narrow-band hypothesis we take $m = 6.985$ ($\beta = 0.02$) and, accordingly, $\beta = 0.041$ and $\nu = 0.241$. In the linear filtering method [see, e.g., Borgman, 1969], the surface elevation is given by

$$\varsigma(t) = \int_{-\infty}^{\infty} h(\tau) w(t - \tau) d\tau = h(t) * w(t), \quad (75)$$

where $w(t)$ is the white-noise signal, and

$$h(t) = F^{-1}\left\{\sqrt{S(\omega)/2}\right\}, \quad (76)$$

in which F^{-1} denotes the Fourier inverse transform and $S(\omega)$ is the target spectrum (one side). From equations (75) and (76) we have

$$Z(\omega) = W(\omega) \sqrt{S(\omega)/2}, \quad (77)$$

where

$$Z(\omega) = F\{\varsigma(t)\} \quad W(\omega) = F\{w(t)\}, \quad (78)$$

with F denoting the Fourier transform.

[44] In practical computation, the Wallops spectrum shown in equation (74) with $\omega_0 = 1.07$ rad/s and $m = 6.985$ is taken as the target spectrum and the FFT algorithm is used to make the computation fast and efficient. The sequence $S(\omega_n)$, $n = 0, 1, 2, \dots, N - 1$ is obtained by

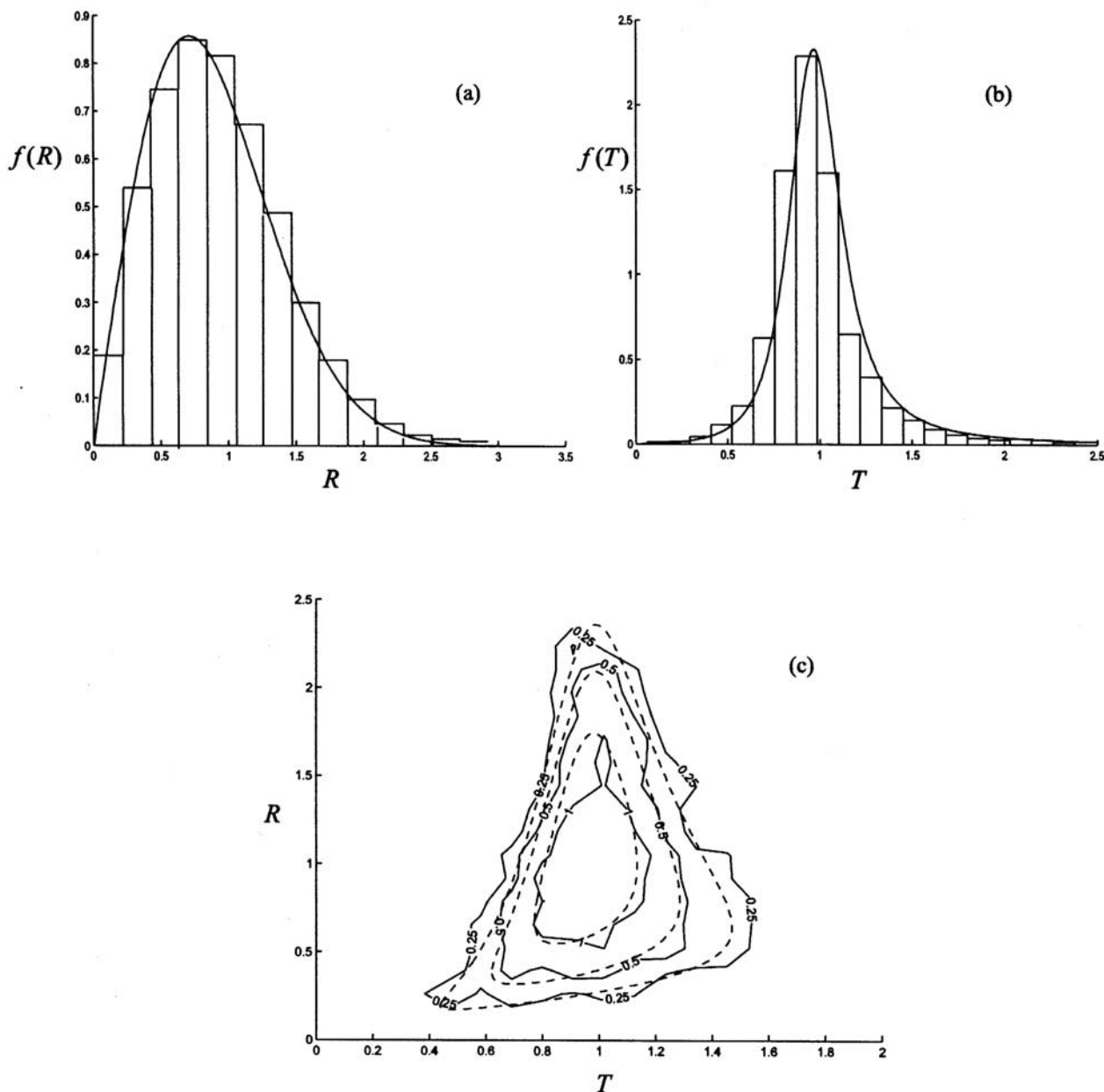


Figure 6. Comparisons between the numerically simulated distributions and their corresponding theoretical distribution. (a) $R(t)$, (b) $T(t)$, and (c) the joint distribution of $R(t)$ and $T(t)$.

digitizing $S(\omega)$ (double-sided) truncated at $\pm 18 \omega_p$, and the random numbers with distribution of $N(0, 1)$ is created by computer to close with the sequence $W(t)$ and then obtain $W(\omega_n)$ through equation (78), $n = 0, 1, 2, \dots, N - 1$ ($N = 2 \times 10^4$). From $S(\omega_n)$ and $W(\omega_n)$ we obtain $Z(\omega_n)$ through equation (77) and then the simulated signal $\zeta(t_n)$, $n = 0, 1, 2, \dots, N - 1$ ($\Delta t = 0.025$) through IFFT. The local amplitude $\rho(t_n)$ and local period $\tau(t_n)$ are measured from $\zeta(t_n)$ by the Hilbert transform technique, which will be outlined in the following subsection. Figure 6 shows the distribution histograms of $R(t)$ and $T(t)$, the joint distribution counters of $R(t)$ and $T(t)$, and their corresponding theoretical PDFs given by equations (24), (46), and (18), respectively. As can be seen from Figures 6a, 6b, and 6c, the agreements between

simulated distributions and theoretical ones are well satisfactory, as expected.

4.2. Laboratory Experiment I

[45] This experiment is performed in a covered flume of Physical Oceanography Laboratory, Ocean University of China. The flume is 65 m long, 1.5 m wide and 1.5 m high. The waves in the flume are generated by stable and uniform winds that are produced by a wind-blower system joined with a rectifying channel. The water in the flume was 0.75 m deep during the experiment.

[46] By a capacitance-type wave gauge the surface elevation $\zeta(t)$ is measured at a point with fetch = 30 m and at $U = 7, 9$ and 11 ms^{-1} , where the fetch is referred to

the distance from the wind issue to the point, and U denotes the reference wind speed. Three records, each being 5 min long, are obtained and sampled at $\Delta t = 0.02$ s. The number of sample, N , is 15000 for each record.

[47] The local wave period $\tau(t_n)$, $n = 1, 2, \dots, N$, is computed from $\zeta(t_n)$ by applying the Hilbert transform technique that has been extensively and effectively employed to measure the local wave variables, such as the local wave height, period and phase, from a wave record with narrow spectrum (see section 1). This technique is briefly outlined in the following.

[48] In accordance with the properties of the Hilbert transform [e.g., Papoulis, 1984], it is easy to show from equation (6) that

$$F\{W(t)\} = \begin{cases} 2F\{\zeta(t)\} & \omega > 0 \\ 0 & \omega < 0 \end{cases}, \quad (79)$$

where

$$W(t) = \zeta(t) + i\xi(t). \quad (80)$$

From equations (79) and (80) it is seen that the Hilbert transform $\xi(t)$ can be computed from the record $\zeta(t)$ through the Fourier transform and its inversion. The FFT algorithm makes the computation highly efficient. The local amplitude $\rho(t)$ and phase $\varphi(t)$ are given by equations (8) and (9), respectively, and the local wave period $\tau(t)$ is given by

$$\tau(t) = \frac{2\pi}{|\dot{\varphi}(t)|}. \quad (81)$$

[49] To make the wave records close to the condition of the narrow-band hypothesis adopted in deriving the present PDFs, we band pass the records by a method that is an improvement of the Fourier series method presented by Longuet-Higgins [1984] for band passing a wave record. In order to move out, from a record, the sinusoidal components with frequencies outside the range $(\omega_{n'}, \omega_{n''})$, where n' and n'' are two numbers such that $0 < \omega_{n'} < \omega_{n''} < \omega_{N/2}$ with $\omega_{N/2}$ as the Nyquist frequency, we change equation (79) into

$$F\{\tilde{W}(t)\} = \begin{cases} 0 & \omega < \omega_{n'} \text{ and } \omega > \omega_{n''} \\ 2F\{\zeta(t)\} & \text{otherwise} \end{cases}. \quad (82)$$

It is easy to show that the real and imaginary parts of $\tilde{W}(t)$ are the filtered record $\tilde{\zeta}(t)$ and its Hilbert transform $\tilde{\xi}(t)$, respectively, namely,

$$\left. \begin{aligned} \tilde{\zeta}(t) &= \text{Re } \tilde{W}(t) \\ \tilde{\xi}(t) &= \text{Im } \tilde{W}(t) \end{aligned} \right\}, \quad (83)$$

and the local amplitude and wave period of $\tilde{\zeta}(t)$ are given by

$$\tilde{\rho}(t) = [\tilde{\zeta}^2(t) + \tilde{\xi}^2(t)]^{1/2}, \quad (84)$$

$$\tilde{\tau}(t) = \frac{2\pi}{|\dot{\tilde{\varphi}}(\omega)|}, \quad (85)$$

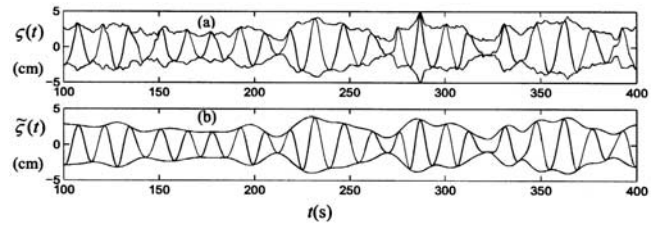


Figure 7. (a) A typical section of the original record and its local amplitude computed by the Hilbert transform technique. (b) The corresponding filtering record and its local amplitude computed by the FFT filtered method. The record is measured at $U = 9$ ms^{-1} and fetch = 30 m.

where

$$\tilde{\varphi}(\omega) = \arctan\left\{\frac{\tilde{\xi}(t)}{\tilde{\zeta}(t)}\right\}. \quad (86)$$

As the improved method can be employed to fast and efficiently band pass a wave record by using the FFT algorithm, it is referred to as the FFT filtering method.

[50] In this experiment the passband of filtering is chosen to be

$$0.3\omega_p < \omega < 2.0\omega_p, \quad (87)$$

where ω_p denotes the peak frequency of the spectrum estimated from a record. Figure 7 gives an example of band passed record; Figure 7a shows a typical section of the original record measured at $U = 9$ ms^{-1} and fetch = 30 m, and its local amplitude computed by the Hilbert transform technique described in equations (79), (80), and (8), while Figure 7b shows the corresponding filtered record and its local amplitude computed by the FFT filtering method with the passband taken to be $0.3\omega_p < \omega < 2.0\omega_p$.

[51] For convenience in reporting the experiment, we first introduce some denotations: $\zeta(t_n)$, the original record measured at $U = 9$ ms^{-1} and fetch = 30 m in this experiment; $\tilde{\zeta}(t_n)$, the filtered record computed from $\zeta(t_n)$ by the FFT filtering method with the passband chosen to be $0.3\omega_p < \omega < 2.0\omega_p$; $\rho(t_n)$ and $\tau(t_n)$, the local amplitude and period of $\zeta(t_n)$ computed by the Hilbert transform technique; $\tilde{\rho}(t_n)$ and $\tilde{\tau}(t_n)$, the local amplitude and period of $\tilde{\zeta}(t_n)$ computed by the FFT filtered method; m_n and \tilde{m}_n , the n th moments of the spectrum estimated from $\zeta(t_n)$ and $\tilde{\zeta}(t_n)$, respectively; $R(t_n) = \rho(t_n)/(2m_0)^{1/2}$; $\tilde{R}(t_n) = \tilde{\rho}(t_n)/(2\tilde{m}_0)^{1/2}$; $T(t_n) = \tau(t_n)/(2\pi m_0/m_1)$; $\tilde{T}(t_n) = \tilde{\tau}(t_n)/(2\pi \tilde{m}_0/\tilde{m}_1)$; $\nu = (m_0 m_2/m_1^2 - 1)^{1/2}$; $\tilde{\nu} = (\tilde{m}_0 \tilde{m}_2/\tilde{m}_1^2 - 1)^{1/2}$; $h(t_n) = 2\rho(t_n)$; $\tilde{h}(t_n) = 2\tilde{\rho}(t_n)$; \bar{h} and $\tilde{\bar{h}}$, the averaged local wave height computed from $\zeta(t_n)$ and $\tilde{\zeta}(t_n)$, respectively; $h_{1/3}$ and $\tilde{h}_{1/3}$, the significant wave heights computed from $\zeta(t_n)$ and $\tilde{\zeta}(t_n)$, respectively; $H_{1/3} = h_{1/3}/\bar{h}$; and $\tilde{H}_{1/3} = \tilde{h}_{1/3}/\tilde{\bar{h}}$.

[52] The results computed from the three records measured in the experiment are quite similar. To save space, only those computed from the record measured at $U = 9$ ms^{-1} and fetch = 30 m will be shown as examples in the following. The parametric values computed from the record are listed in Table 1.

[53] Figures 8a and 8b respectively show the experimental joint distribution counters of $\tilde{R}(t_n)$ and $\tilde{T}(t_n)$ and of $R(t_n)$

Table 1. Parametric Values Computed From the Record Measured at $U = 9 \text{ ms}^{-1}$ and Fetch = 30 m

Parameter	Unit	Value
m_0	cm^2	2.56
\tilde{m}_0	cm^2	2.49
m_1	$\text{cm}^2 \text{ s}^{-1}$	24.5
\tilde{m}_1	$\text{cm}^2 \text{ s}^{-1}$	23.3
m_2	$\text{cm}^2 \text{ s}^{-2}$	248
\tilde{m}_2	$\text{cm}^2 \text{ s}^{-2}$	223
ν	cm	0.237
$\tilde{\nu}$	cm	0.147
\bar{h}	cm	4.28
\tilde{h}	cm	4.16
$H_{1/3}$	cm	1.51
$\tilde{H}_{1/3}$	cm	1.63

and $T(t_n)$, and their corresponding theoretical counters given by equation (18). As is seen, the distribution mode in Figure 8a is somewhat different from that in Figure 8b. This is because $\tilde{\nu}$ and ν have different values, as can be seen from Table 1.

[54] Figure 9 shows the histograms of conditional distributions of $\tilde{T}(t_n)$ assuming $\tilde{h}_{1/3}$ and of $T(t_n)$ assuming $H_{1/3}$, and their corresponding theoretical curves given by equation (33). Figure 10 shows the histograms of $\tilde{\tau}(t_n)$ and of $\tau(t_n)$, and their corresponding theoretical curves given by equation (48).

[55] From Figures 8, 9, and 10 we see the common features: (1) The theoretical distributions agree, to a great extent, with the empirical distributions, and (2) The agreements between the theoretical and empirical distribution curves computed from the filtered record $\zeta(t_n)$ are better than those computed from the original record $\zeta(t_n)$, as expected.

4.3. Laboratory Experiment II

[56] This experiment is performed in the same flume as that described in section 4.2. The surface elevation $\zeta(t)$ is

measured at fetch = 30 m simultaneously by two wave probes being 7.5 cm apart along the flume. Two pairs of synchronous records are obtained at $U = 9$ and 11 ms^{-1} . Each of these records is 10 min long and sampled at $\Delta t = 0.05 \text{ s}$ ($N = 12000$). All of these records are band passed by the FFT filtering method with the passband chosen to be $0.3\omega_p < \omega < 2.0\omega_p$. As the passband is so narrow and the distance between the two probes is so small, the corresponding condition of the band passed records is considered to be close to the condition assumed in deriving the theoretical PDF (73).

[57] The instantaneous wavelength $\lambda(t_n; x)$, $n = 1, 2, \dots, N$, are computed from a pair of records according to the formula

$$\left. \begin{aligned} \lambda(t_n; x) &= \frac{2\pi}{k(t_n; x)} = \frac{2\pi\Delta x}{\varphi(t_n; x + \Delta x/2) - \varphi(t_n; x - \Delta x/2)} \\ n &= 1, 2, \dots, N \end{aligned} \right\}, \quad (88)$$

$$\varphi(t_n; x \pm \Delta x/2) = \arctan \left[\frac{\xi(t_n; x \pm \Delta x/2)}{\zeta(t_n; x \pm \Delta x/2)} \right]$$

where x is regarded as a position parameter, $k(t; x)$ represents the instantaneous wave number, and $\xi(t; x)$ is the Hilbert transform of the record $\zeta(t; x)$, defined as

$$\xi(t; x) = \frac{1}{\pi} \int_{-\infty}^{\infty} \frac{\zeta(\tau; x)}{t - \tau} d\tau. \quad (89)$$

This formula has been frequently employed to compute the instantaneous wavelength from a pair of wave records with narrow spectra measured at suitably separated two points [e.g., Melville, 1983; Hwang *et al.*, 1989; Stansell and MacFanlane, 2002]. In the present experiment, x refers to the point with fetch = 30 m and Δx is 7.5 cm.

[58] Still we shall merely show the results computed from the records measured at $U = 9 \text{ ms}^{-1}$ and fetch = 30 m as examples in the following. Figure 11a shows the histogram

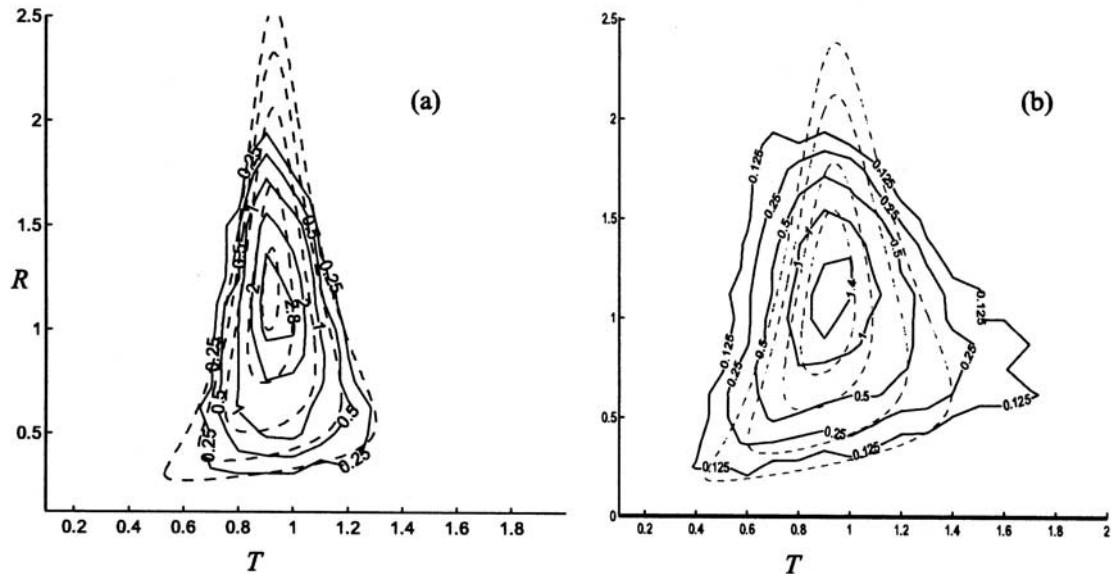


Figure 8. Comparison between the empirical joint distribution counters (solid curves) and its corresponding theoretical counters (dashed curves). (a) The joint distribution of $\tilde{R}(t_n)$ and $\tilde{T}(t_n)$ and its corresponding theoretical distribution. (b) The joint distributions of $R(t_n)$ and $T(t_n)$ and its corresponding theoretical distributions.

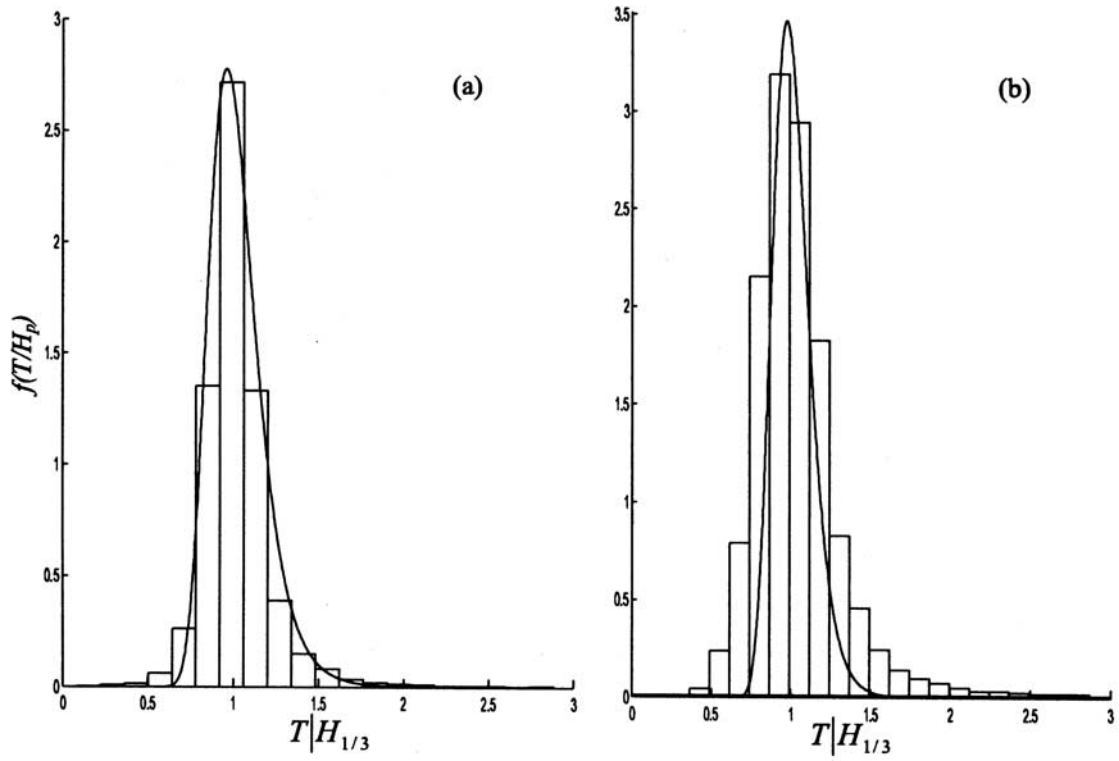


Figure 9. (a) The histogram of $\tilde{T}(t_n)|\tilde{H}_{1/3}$ and its corresponding theoretical curves. (b) The histograms of $T(t_n)|H_{1/3}$ and its corresponding theoretical curves. The theoretical curves are given by equation (33).

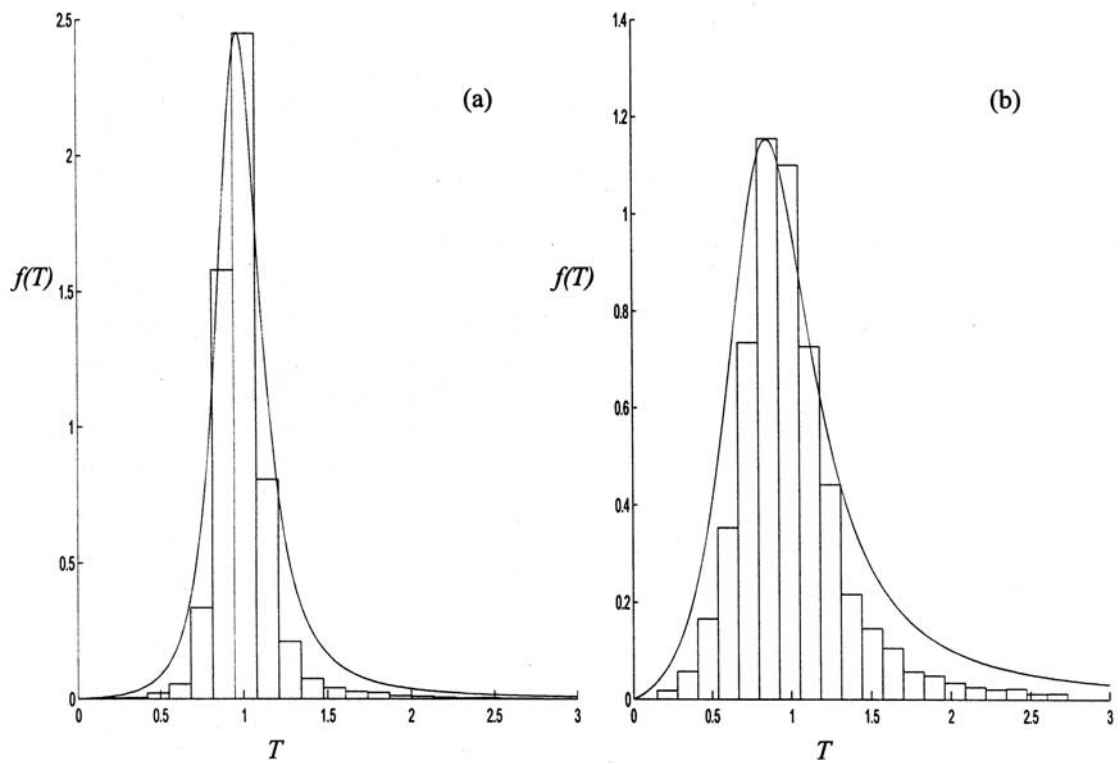


Figure 10. (a) The histogram of $\tilde{\tau}(t_n)$ and its corresponding theoretical curve. (b) The histogram of $\tau(t_n)$ and its corresponding theoretical curve. The theoretical curves are given by equation (48).

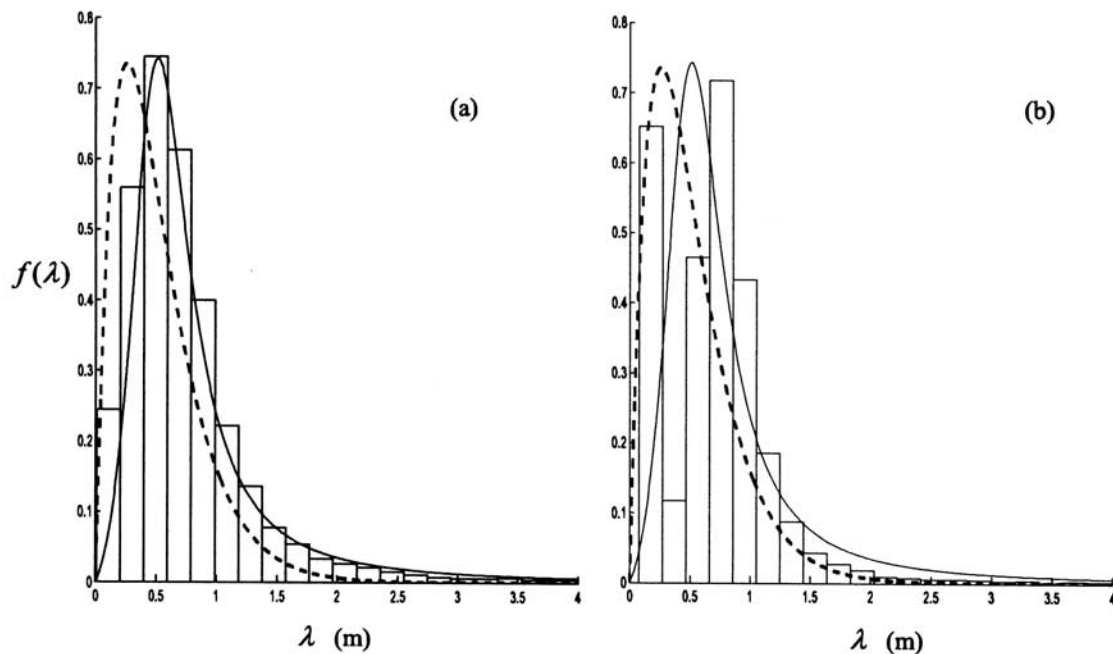


Figure 11. Histogram of λ indirectly measured from two synchronous wave records: (a) from the filtered records and (b) from the original records. The solid and dashed curves represent the distributions given by the present PDF (73) and the empirical Rayleigh PDF (56), respectively.

of $\lambda(t_n; x)$ computed from the filtered records and its corresponding theoretical curve given by equation (73) in which the values of m_n are estimated from one of the filtered records, while Figure 11b shows the histogram of $\lambda(t_n; x)$ computed from the original records and its corresponding theoretical curves given by equation (73) in which the values of m_n are estimated from one of the original records. Also shown in Figures 11a and 11b are the corresponding Rayleigh curves given by the empirical PDF

$$f_R(\lambda) = \frac{\pi}{2} \frac{\lambda}{\bar{\lambda}^2} \exp\left\{-\frac{\pi}{4} \left(\frac{\lambda}{\bar{\lambda}}\right)^2\right\}, \quad (90)$$

where the averaged instantaneous wave height is taken as $\bar{\lambda}$. This PDF has been employed to derive the well-known Bretschneider spectrum of sea waves [Bretschneider, 1959]. As can be seen, Figure 11a the theoretical curve gives a fairly good fit to the histogram, as expected, while in Figure 11b the fit is quite poor. For the latter our explanation is that, on one hand, both the phase functions $\varphi(t_n; x - \Delta x/2)$ and $\varphi(t_n; x + \Delta x/2)$ computed from the original records of wind waves are rapidly fluctuated, as can be seen from Figure 7, so that they can not be expected to result in well reasonable $\lambda(t_n; x)$ and that, on the other hand, the condition assumed in the derivation of equation (73) deviates from the condition of laboratory wind waves. We attribute the anomalous rising at the left end of the histogram in Figure 11b to the measurement method and the chosen distance (7.5 cm) between the two probes. It is worth mentioning that if the distance was chosen to be less than 7.5 cm, the two wave probes would considerably interfere each other. As can also be seen, the empirical Rayleigh distribution substantially deviates from the histogram both in Figures 11a and 11b.

[59] As well known, it is difficult to estimate m_4 from a wind-wave record because the spectrum estimated from the

record has a ill tail that makes the computed m_4 so large that the resulting ε is always close to 1. To overcome the difficulty, we have to perform the time-smoothing [see, e.g., Glazman, 1986] on both the original and filtered records:

$$\tilde{\zeta}(t) = \frac{1}{T} \int_{t-T/2}^{t+T/2} \zeta(t) dt, \quad (91)$$

where T is the smoothing scale. This time-smoothing is equivalent to multiplying the spectrum estimated from a record by the smoothing function

$$W(\omega T) = [\sin(\omega T/2)/(\omega T/2)]^2. \quad (92)$$

The smoothing scale T is chosen to be the Taylor microscale, namely, $T = (m_0/m_2)^{1/2}$, as suggested by Glazman [1986]. The values of m_n , μ , and $\bar{\lambda}$ computed from the smoothed records are listed in Table 2. These values, as parametric ones, have been used in computing the theoretical curves from equation (73).

5. Conclusions

[60] We have derived the PDF (18) or (22) for the joint distribution of wave heights and periods and the PDF (68) for the joint distribution of wave heights and wavelengths. While based also on a Gaussian process under the narrow-spectrum hypothesis, the derivation of equation (18), unlike that in the work of Longuet-Higgins [1975] nor that of Longuet-Higgins [1983], is in virtue of an approximate Hilbert transform that is legitimate to this hypothesis and has been widely employed to measure local wave variables from a wave record with narrow spectrum. The joint PDF (18) has the following advantages: (1) it is almost the same in magnitude as the joint PDF in the work of Longuet-Higgins [1983] that has been shown to give a good fit to

Table 2. Values of m_n , μ , and $\bar{\lambda}$ Computed From the Smoothed Wave Records

	m_0 , cm ²	m_2 , cm ² s ⁻²	m_4 , cm ² s ⁻⁴	μ ,	$\bar{\lambda}$, cm
Original record	1.02	107	1.46×10^4	0.548	87.4
Filtered record	1.01	104	1.14×10^4	0.253	74.0

sea-wave data with a narrow spectrum; (2) depending only on the parameter ν the present joint PDF is considerably simpler in form than that in the work of *Longuet-Higgins* [1983] and produces an exactly Rayleigh distribution of wave heights rather than the slightly non-Rayleigh distribution as in the work of *Longuet-Higgins* [1983]. This simpler solution has led to the relatively simple PDF (33) for the conditional distribution of wave periods assuming the wave height and to the relatively simple PDF (48) for the distribution of wave period. From the former we have predicted several typical conditional statistics of sea-wave periods, which may be useful to scientific and engineering applications.

[61] The derivation of the joint PDF (68) is also in virtue of the approximate Hilbert transform but based on a unidirectional and homogeneous Gaussian wave field with narrow spectrum. It has been found that for such a wave field the joint PDF of wave height and wavelength depends only on the parameter $\mu = (m_0 m_4 / m_2^2 - 1)^{1/2}$. From this joint PDF we have obtained the PDF (73) of wavelength, which is perhaps the first theoretical PDF proposed for the distribution of wavelengths of sea waves.

[62] The numerical simulation experiment has shown the PDFs (18) or (22), (24) or (26) and (46) give well satisfactory fits to the data simulated with a narrow-band Wallops spectrum as target. The experiments of laboratory wind waves have shown that the PDFs (18), (33) and (48) give fairly good fits to their corresponding histograms and counters resulting from the band passed wave records and also that these PDFs agree to a great extent with the histograms and counters resulting from the original records of wind waves. The experiments have also shown that the agreement between the PDF (73) and its corresponding histograms is fairly good for the filtered records but is rather poor for the original records, as shown in Figure 11b. We attribute the disagreement to the difference in conditions as well as the limitation of the method described in equation (83) by which we measured the wavelength in the experiment.

Appendix A: Derivation of $f(\rho, j)$

[63] In accordance with the properties of the Hilbert transform of a stationary process [see, e.g., *Papoulis*, 1984], it is easy to show R_{ij} in equation (12) to be

$$\left. \begin{aligned} R_{12} = R_{21} = R_{13} = R_{31} = R_{24} = R_{42} = R_{34} = R_{43} = 0 \\ R_{11} = R_{22} = m_0, \quad R_{14} = R_{41} = m_1, \quad R_{23} = R_{32} = -m_1, \\ R_{33} = R_{44} = m_2 \end{aligned} \right\} \quad (A1)$$

It follows from equations (12) and (A1) that

$$D = (m_0 m_2 - m_1^2) \equiv \Delta^2, \quad (A2)$$

and then from equation (10) that

$$f(\varsigma, \xi, \dot{\varsigma}, \dot{\xi}) = \frac{1}{(2\pi)^2 \Delta} \exp \left\{ -\frac{1}{2\Delta} \left[m_2 (\varsigma^2 + \xi^2) + m_0 (\dot{\varsigma}^2 + \dot{\xi}^2) + 2m_1 (\xi \dot{\varsigma} - \varsigma \dot{\xi}) \right] \right\} \quad (A3)$$

The joint PDF of ρ , φ , $\dot{\rho}$ and $\dot{\varphi}$ is found by

$$f(\rho, \varphi, \dot{\rho}, \dot{\varphi}) = f(\varsigma, \xi, \dot{\varsigma}, \dot{\xi}) \frac{\partial(\varsigma, \xi, \dot{\varsigma}, \dot{\xi})}{\partial(\rho, \varphi, \dot{\rho}, \dot{\varphi})}. \quad (A4)$$

From equations (3) and (7) we have

$$\begin{aligned} \dot{\varsigma}(t) &= \dot{\rho}(t) \cos \varphi(t) - \rho(t) \dot{\varphi}(t) \sin \varphi(t) \\ \dot{\xi}(t) &= \dot{\rho}(t) \sin \varphi(t) + \rho(t) \dot{\varphi}(t) \cos \varphi(t) \end{aligned}$$

and then

$$\frac{\partial(\varsigma, \xi, \dot{\varsigma}, \dot{\xi})}{\partial(\rho, \varphi, \dot{\rho}, \dot{\varphi})} = \rho^2. \quad (A5)$$

Thus

$$f(\rho, \varphi, \dot{\rho}, \dot{\varphi}) = \frac{\rho^2}{(2\pi)^2 \Delta} \exp \left\{ -\frac{1}{2\Delta} \left[m_1 \rho^2 + m_0 (\dot{\rho}^2 + \rho^2 \dot{\varphi}^2) - 2m_1 \rho^2 \dot{\varphi}^2 \right] \right\}. \quad (A6)$$

Integration of the above joint PDF with respect to $\dot{\rho}$ from $-\infty$ to $+\infty$ and to φ from 0 to 2π results in equation (13).

[64] **Acknowledgments.** We are very grateful for the sponsorships of our work provided by the National Natural Science Foundation of China under grant 40276006 and by the National 863 program under grant 2002AA-633100.

References

- Bitner-Gregersen, E. M., and S. Gran (1983), Local properties of sea waves derived from a wave record, *Appl. Ocean Res.*, 5, 210–214.
- Borgman, L. E. (1969), Ocean wave simulation for engineering design, *J. Waterways Harbors Div.*, 95(WW4), 557–583.
- Bretschneider, C. L. (1959), Wave variability and wave spectra for wind-generated gravity waves, *Tech. Memo.*, 118, U.S. Beach Erosion Board, Washington, D. C.
- Cartwright, D. E., and M. S. Longuet-Higgins (1956), The statistical distribution of the maxima of a random function, *Proc. R. Soc. London A*, 237(1209), 212–232.
- Cavanič, A., M. Arthan and R. Ezraty (1976), A statistical relationship between individual heights and periods of storm waves, in *Proceedings of the Conference on Behavior Offshore Structures*, pp. 354–360, Norwegian Inst. of Technol., Trondheim.
- Chakrabarti, S. K., and R. P. Coolley (1977), Statistical distribution of periods and heights of ocean waves, *J. Geophys. Res.*, 82, 1363–1368.
- Cox, C. S., and W. H. Munk (1954), Statistics of sea surface derived from sun glitter, *J. Mar. Res.*, 13, 198–227.
- Glazman, R. E. (1986), Statistical characterization of sea surface for a wave slope field discontinuous in the mean square, *J. Geophys. Res.*, 91(C5), 8629–8641.
- Goda, Y. (1978), The observed joint distribution of periods and heights of sea waves, in *Proceedings of the 16th International Conference on*

- Coastal Engineering, Sydney, Australia*, pp. 227–246, Am. Soc. of Civ. Eng., Reston, Va.
- Huang, N. E., and S. R. Long (1980), An experimental study of the surface elevation probability distribution and statistics of wind generated waves, *J. Fluid Mech.*, *101*, 179–200.
- Huang, N. E., R. Long, C. C. Tung, Y. Yuan, and L. F. Bliven (1981), A unified two-parameter wave spectral model for a general sea state, *J. Fluid Mech.*, *101*, 179–200.
- Huang, N. E., S. R. Long, C.-C. Tung, Y. Yuan, and L. F. Bliven (1983), A non-Gaussian statistical model for surface elevation of nonlinear random wave field, *J. Geophys. Res.*, *88*, 7597–7606.
- Hwang, P. A., D. Xu, and J. Wu (1989), Breaking of wind-generated waves: Measurements and characteristics, *J. Fluid Mech.*, *202*, 177–200.
- Lindgren, G. (1972), Wavelength and amplitude in Gaussian noise, *Adv. Appl. Probab.*, *4*, 81–108.
- Lindgren, G., and I. Rychlik (1982), Wave characteristic distribution for Gaussian waves—Wavelength, amplitude and steepness, *Ocean Eng.*, *9*, 411–432.
- Longuet-Higgins, M. S. (1952), On the statistical distribution of the height of sea waves, *J. Mar. Res.*, *11*(3), 245–266.
- Longuet-Higgins, M. S. (1957), The statistical analysis of a random moving surface, *Philos. Trans. R. Soc. London A*, *249*, 321–387.
- Longuet-Higgins, M. S. (1963), The effect of non-linearities on statistical distributions in the theory of sea waves, *J. Fluid Mech.*, *16*, 459–480.
- Longuet-Higgins, M. S. (1975), On the joint distribution of the periods and amplitudes of sea waves, *J. Geophys. Res.*, *80*(18), 2688–2694.
- Longuet-Higgins, M. S. (1983), On the joint distribution of wave periods and amplitudes in a random wave field, *Proc. R. Soc. London A*, *389*, 241–258.
- Longuet-Higgins, M. S. (1984), Statistical properties of wave groups in a random sea state, *Philos. Trans. R. Soc. London A*, *312*, 219–250.
- Melville, W. K. (1983), Wave modulation and breakdown, *J. Fluid Mech.*, *128*, 489–506.
- Papoulis, A. (1984), *Probability, Random Variables, and Stochastic Processes*, 2nd ed., 356 pp., McGraw-Hill, New York.
- Rice, S. O. (1945), Mathematical analysis of random waves, *Bell Syst. Tech. J.*, *24*, 86–156.
- Shum, K. T., and W. K. Melville (1984), Estimates of the joint statistics of amplitudes and periods of ocean waves using an integral transform technique, *J. Geophys. Res.*, *89*(C4), 6469–6476.
- Srokosz, M. A. (1986), On the probability of wave breaking in deep water, *J. Phys. Oceanogr.*, *16*, 382–385.
- Stansell, P., and C. MacFarlane (2002), Experimental investigation of wave breaking criteria based on wave phase speeds, *J. Phys. Oceanogr.*, *32*(5), 1269–1283.
- Sun, F. (1988), Statistical distribution of variables of 3-D ocean waves (in Chinese), *Chin. Sci., Ser. A*, *5*, 501–508.
- Tayfun, M. A. (1980), Narrow-band nonlinear sea waves, *J. Geophys. Res.*, *85*(3), 1548–1552.

X. Li, H. Lu, D. Xu, N. Xu, and L. Zhang, Physical Oceanography Laboratory, Ocean University of China, Qingdao 266003, China. (xudel@mail.ouc.edu.cn)